Available online at www.sciencedirect.com

ScienceDirect

Structural Integrity Procedia 00 (2022) 000–000

Structural Integrity Procedia

www.elsevier.com/locate/procedia

XIX ANIDIS Conference, Seismic Engineering in Italy

Study on the effectiveness of a CRM system: in-plane and out-of-plane cyclic tests on masonry piers

N. Gattesco[a], E. Rizzi[a]*, A. Bez[a], A. Dudine[b]

[a]*University of Trieste, Department of Engineering and Architecture, Via Alfonso Valerio 6/1, 34127 Trieste, Italy*

[b] *Fibre Net S.p.A.. Via Jacopo Stellini 3, Z.I.U. 33050 Pavia di Udine (UD), Italy*

Abstract

The results of a broad experimental campaign on full scale masonry samples are presented in the paper, to evidence the effectiveness of a CRM (Composite Reinforced Mortar) strengthening System. In particular, shear-compression tests were carried out on masonry samples strengthened with the application of the CRM System on one or both faces of the wall, consisting of a mortar coating reinforced with a preformed GFRP (Glass Fiber Reinforced Polymer) mesh. In the former case, to connect wall leaves, artificial diatones were used; in the latter case, these diatones and couples of GFRP L-shape connectors were used to confine the masonry wall. The three-point bending test was also carried out on one-side reinforced masonry specimen, in which also artificial diatones were used. The sample was arranged vertically and loaded cyclically according to a three-point bending scheme. The results of all reinforced specimen tests were compared with those of the equivalent unreinforced ones.

Peer-review under responsibility of the scientific committee of the XIX ANIDIS Conference, Seismic Engineering in Italy

Keywords: CRM reinforcement, jacketing strenghtened masonry, seismic vulnerability, masonry experimental tests, existing masonry structure

1. Introduction

Stone masonry constructions are an important part of the existing buildings in many Italian regions. The most of them are made with irregular elements connected with poor lime mortar, and for this reason there are many existing buildings that are seismically inadequate. Different strengthening techniques were proposed over the last few decades, to reduce the vulnerability of buildings. Shear-compression tests (Mercedes et al., 2020, Garcia-Ramonda et al., 2022,

* Corresponding author. Tel.: +39 339 7057482.
E-mail address: emanuele.rizzi@units.it

Peer-review under responsibility of the scientific committee of the XIX ANIDIS Conference, Seismic Engineering in Italy

Guerreiro et al., 2018) and out-of-plane bending tests (Ismail and Ingham, 2016, De Santis et al., 2019) were carried out on these systems. Amongst all, in the present research a deep study on the CRM (Composite Reinforced Mortar) strengthening technique is proposed. This consists in applying on one or two sides of the masonry wall a mortar coating, in which a GFRP (Glass Fiber Reinforced Polymer) mesh is embedded. The GFRP consists of Alkali-Resistant-glass fibers and an epoxy vinyl ester resin, thus becoming a pre-formed high resistant core. The GFRP mesh is embedded in a mortar coating and applied to the masonry surface through GFRP connectors. This type of reinforcement is useful to increase the load-bearing capacity and the ductility of the element. Moreover, it allows the distribution of damage resulting in a more consistent energy dissipation. However, the intervention does not affect sensibly the distribution of masses in the structure, since the total thickness of the mortar coating is only 30 mm. To further improve the behavior of the masonry, in the case of a multi-leaf configuration and with one-side reinforcement, diatones have to be included in the operation (the importance of the transversal connection was previously underlined by(Cascardi et al., 2020; Gattesco et al., 2013). The diatones are made of stainless-steel bars, which are inserted into the wall and fixed to the masonry through a cementitious thixotropic grout. To contrast the detachment of the reinforced coating, a hollow steel washer is embedded in it. The diatones allows to reach significant resistance and deformation capacity improvements in one side masonry reinforcement, differently to what found by other authors (Valluzzi et al., 2001) without using diatons.

To learn more about the behavior of this reinforcement, several experimental tests were carried out within the present research. Particularly, in this paper a series of in-plane shear-compression tests and a three-point bending out-of-plane test on piers will be presented. The experimental campaign has been carried out in the Materials and Structures Testing Laboratory of the University of Trieste.

2. General description of the experimental campaign

The performed tests are summarized in the Table 1. For the shear-compression test, the unreinforced specimen was firstly considered, to assess the structural effectiveness of each type of reinforcement considering the subsequent tests. For the three-point bending test, the efficiency of the reinforcement was evaluated comparing the response of the unreinforced side with that of the reinforced one of the specimens. This is eligible because of the little influence of the reinforced side over the behavior of the wall with the unreinforced side in tension.

Table 1 - Specimen characteristics

Specimen	Type of test	Reinforcement	Reinforcement properties
P-R2U	Shear compression test on two leaf rubble stone specimens, unreinforced	Unreinforced	-
P-R2R-1	Shear compression test on two leaf rubble stone specimens, reinforced on one side	CRM system + diatones	GFRP mesh reinforced mortar coating on one face of the specimen, four "L" connectors, two diatones per m^2
P-R2R-2	Shear compression test on two leaf rubble stone specimens, reinforced on two sides	CRM system	GFRP mesh reinforced mortar coating on both faces of the specimen, six "L" shaped GFRP connectors per m^2
B-R2	Out-of-plane three-point bending test on double leaf rubble stone, reinforced on one side	CRM system + diatones	GFRP mesh on a single face of the specimen, four "L" connectors, two diatones per m^2

3. Materials

The stone masonry specimens were realized with rubble limestone blocks with averaged dimensions 15 x 23 x 9 cm^3. The shear-compression test pier specimens measure 1.50 x 1.96 x 0.35 m^3, whereas the three-point bending test specimens measure 2.48 x 1.03 x 0.25 m^3. Some compression tests carried out on 0.50 x 0.35 x 1 m^3 rubblestone masonry samples at the University of Ljubljana, provided average values for the Young's modulus and the compressive strength equal to $E_{masonry}$ = 1074 MPa and $f_{c,masonry}$ = 2.48 MPa, respectively. The mortar joints are made using 200 kg of hydraulic lime per m^3 of dry mortar. Also in this case, several experimental tests were preliminary carried out on mortar samples, which provided an average compressive strength of $f_{c,mortar}$ = 0.93 MPa and an average tensile strength of $f_{t,mortar}$ = 0.17 MPa.

For the reinforcement, a regular 66x66 mm^2 pattern of the square shape GFRP mesh has been installed. The mesh is constituted by horizontal parallel fibers and vertical twisted fibers wires. The single parallel wire has a cross section of 11.6 mm^2 and the twisted wire has a cross section of 8.9 mm^2. The adopted GFRP mesh (mesh density 420 kg/m^2), in accordance with the technical data provided by the producer, can offer an average Young's modulus $E_{bar} \geq 25$ GPa, an ultimate characteristic tensile resistance $F_{ub,bar} = 4.3$ kN and an ultimate tensile strain $\varepsilon_{u,bar} = 1.45\%$.

A 30 mm thick mortar coating has been applied embedding a GFRP mesh in the middle of the pre-mixed mortar layer. The mortar coating is based on natural hydraulic lime, and, according to the technical data provided by the producer, has an elastic modulus $E_{mortar} \leq 10$ GPa and a compressive strength at 28 days ageing ≥ 15 MPa.

The connection between the reinforced coating and the masonry wall is provided through the application of appropriate connectors, composed of "L-shaped" GFRP elements, in number of six elements per m^2. The adopted connectors have an average ultimate tensile resistance $F_{ub,conn} = 21$ kN and an average Young's modulus $E_{conn} = 21.4$ GPa. For the installation, a passing-through hole (diameter 24mm) is realized on the masonry wall and a superposition of connectors of at least 200mm is guaranteed to lap splice. An injection of thixotropic vinyl-ester resin is used to provide a structural interaction between the connector and the masonry element. Particularly vulnerable points are the intersection between the L-connectors and the GFRP mesh, because of the peak of tension that might occur in that area. For this reason, in addition to the mesh, a further sheet (dim. 150x150 mm^2) of 33x33 mm^2 of GFRP mesh is applied on these critical points to better distribute the stress.

Finally, diatones are made by drilling a 50mm diameter hole with a rotating coring machine water cooled, and by positioning a steel threaded bar M16, injected with high strength thixotropic mortar.

4. Shear Compression Test

4.1. Tests setup and proceedings

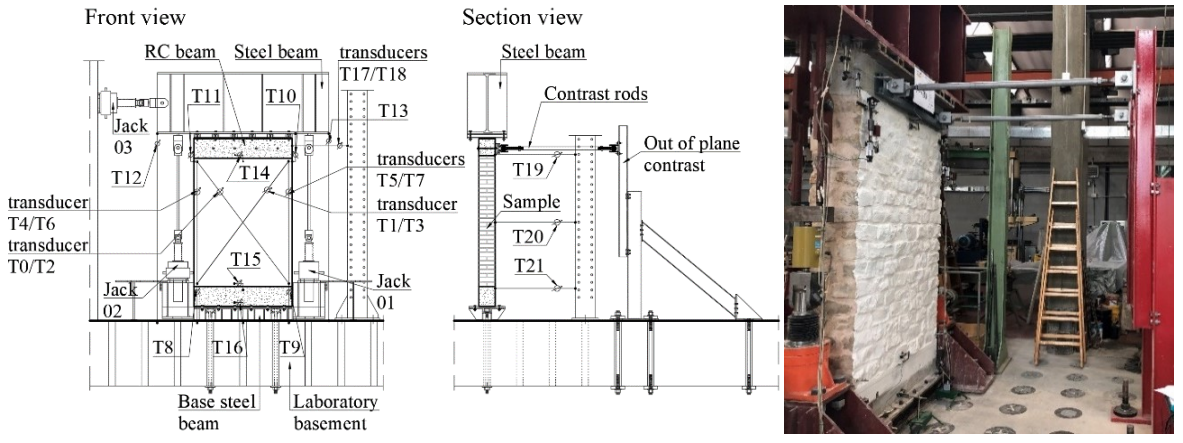

(a) (b) (c)

Fig. 1. Shear compression test setup: a) front drawing of the test element, b) lateral drawing of the test element, c) view of the apparatus.

Each masonry specimen was laid over a reinforced concrete (RC) element (dim. 1.50 x 0.35 x 0.30 m^3); the steel stirrups of the concrete element were welded to a holed steel plate 20 mm thick. The steel plate was connected to a welded steel profile, fixed to the floor by means of a couple of steel tie rods, each pretensioned with a 140 kN force. A second RC element with the same dimensions of the previous one was placed on the top of the masonry specimens and connected to a stiff steel beam, able to apply both vertical and horizontal forces to the tested masonry walls (Fig. 1a). During the tests, the out-of-plane displacements were prevented at the upper RC element level by two steel rods (Fig. 1b). These steel rods were connected to an external support, rigidly fixed to the laboratory floor.

The location of the instruments used during the experimental measures is reported in Fig. 1a: three electro-mechanical actuators, twenty-one transducers and three load cells were used during the tests. The test procedure consisted first in the application of a vertical compression of 0.5 MPa by means of the two vertical electro-mechanical actuators, connected to the top steel beam and to the stiff concrete floor of the laboratory, then with the third electro-

mechanical actuator the horizontal force at the top of the specimens was applied. The twenty-one potentiometer displacement transducers were used to survey, beside the horizontal displacement of the top of the sample, some relative displacements between various points of the specimen. The load cells were used to register the vertical load and the imposed horizontal load. The vertical load was firstly applied and then maintained constant during the test up to failure. The horizontal actuator was moved cyclically with complete inversion, by considering a displacement-controlled test protocol. The experiment was developed by controlling the three actuators, so that the same total vertical load and the same vertical displacements on transducers T12 and T13 are guaranteed during the test.

The horizontal top displacement was varied cyclically between two opposite values and increasing gradually at the end of each cycle. The maximum horizontal displacement considered for these tests is 15 mm for the P-R2U specimen, 37 mm for the P-R2R-1 specimen and 70 mm for the P-R2R-2 specimen.

The specimens were arranged as illustrated in Fig. 2.

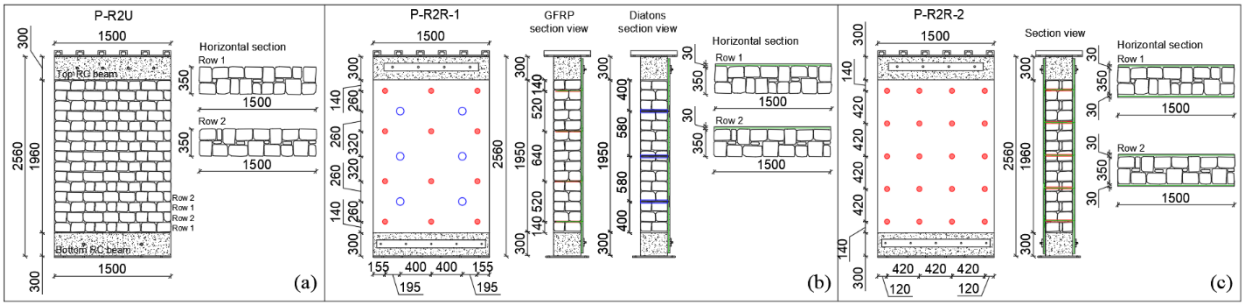

Fig. 2. P-R2U Draft (a), P-R2R-1 Draft (b) and P-R2R-2 Draft (c)

4.2. Results

During the test on specimen P-R2U, a typical progressive crack formation and propagation was observed. Particularly, in both sides of the specimen, the propagation was almost-diagonal. The progressive formation of cracks during different steps on the front side of the specimen is illustrated in Fig. 3a. The specimen reached a maximum shear load H_{max} = 107.8 kN, a maximum lateral displacement at its top end equal to u_p = 15.05 mm ≈0.008h (with *h* the nominal height of the specimen). The conventional ultimate lateral displacement u_u, corresponding at a post-peak residual resistance equal to 80% its maximum resistance H_{max} is equal to 11.4 mm ≈0.006h.

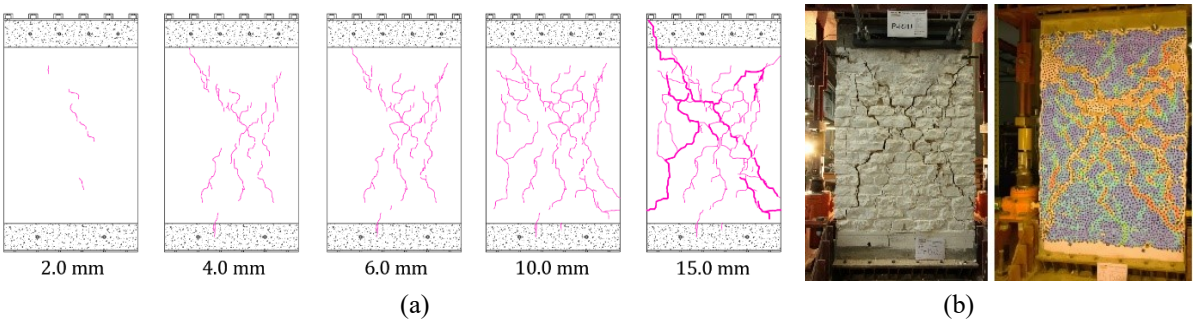

Fig. 3. Crack pattern of the front side during the loading cycles (a), crack pattern at the end of the test on front and rear faces (b)

During the P-R2R-1 specimen test, in the unstrengthened side an initial opening and propagation of vertical cracks in the sample center was observed then the propagation became diagonal. On the strengthened side, the cracks were more distributed in the mortar coating. At the displacement of u=30.0 mm the reinforced coating started detaching also from the center of the wall. After a displacement of u=40.0 mm was reached, the reinforced coating started exfoliating and falling off. The progressive formation of cracks during different steps on the front (strengthened) side of the specimen is reported in Fig. 4. The specimen reached a maximum horizontal force H_{max} = 159.5 kN, a maximum lateral displacement at its top equal to u_p≈0.019h and an ultimate lateral displacement u_u, equal to ≈0.014h (at 80% residual resistance).

In the P-R2R-2 specimen test, it was evidenced a failure mechanism characterized by the combination of compressive and bending stresses, causing a progressive opening and propagation of almost horizontal cracks at the beginning and vertical and diagonal cracks starting from the center of the reinforced coating on the later steps, leading to a subsequent collapse (Fig. 5a). At the displacement of u=16.0 mm the reinforced coating started detaching from the wall in the areas where the cracks were predominant, while at u=30.0 mm the reinforced coating started detaching also from the center of the wall (Fig. 5b). After a displacement of u=40.0 mm was reached, the reinforced coating started exfoliating and falling off. The specimen reached a maximum shear load H_{max} = 229.4 kN, a maximum lateral displacement u_p ≈0.036h and an ultimate lateral displacement u_u, equal to ≈0.025h (measured at 80% residual resistance).

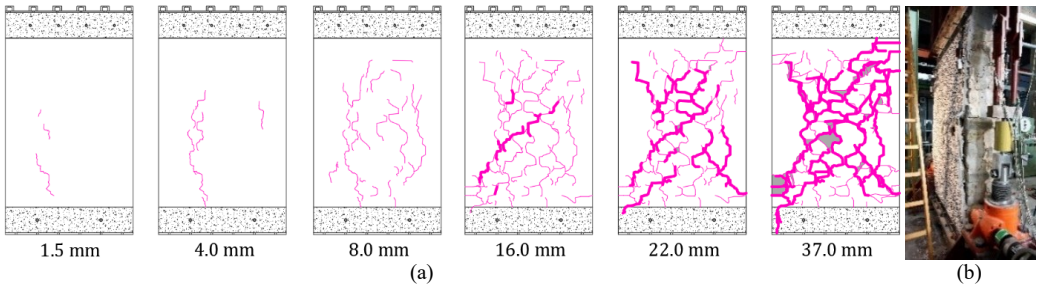

Fig. 4. Crack pattern of the front (strengthened) side during the loading cycles (a), exfoliating of the reinforced coating (b)

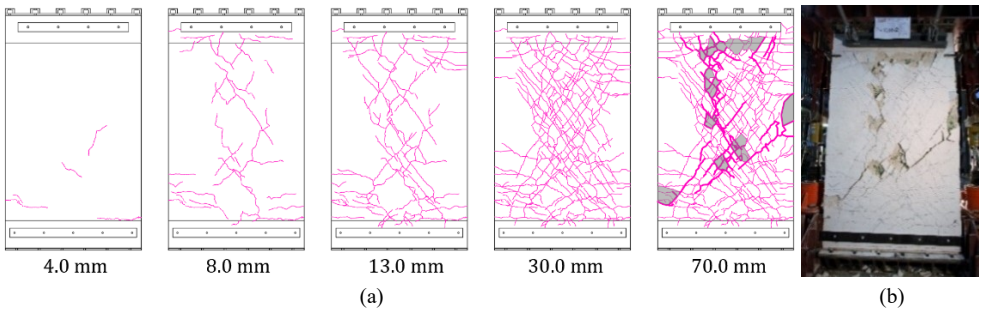

Fig. 5. Crack pattern of the front (strengthened) side during the loading cycles (a), crack pattern at the end of the test (b)

4.3. Discussion on test results

The comparison of the behavior of the three shear-compression tests in terms of shear force against lateral top displacement is useful so to evaluate the effectiveness of the strengthening techniques considered, and it is illustrated in Fig. 6.

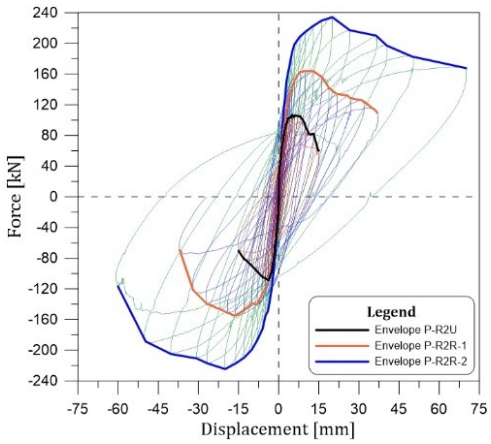

Fig. 6. Shear force (H) against lateral top displacement (u) curve for the three tested specimens

The results obtained from the three shear-compression tests are summarized in the Table 2. In the table: H_{max} is the maximum load reached during the test; u_u *the* ultimate lateral displacement; u_p the displacement corresponding to the maximum load; u_u/h is the corresponding drift. R_{load} represents the ratio between the maximum shear load reached in the strengthened specimen and the maximum load reached in the unreinforced specimen; R_{disp} is the ratio between the ultimate lateral displacement reached in the strengthened specimen and the correspondent lateral displacement reached in the unreinforced one; R_t is the ratio between the equivalent tensile strength of strengthened specimens (calculated according to Gattesco et al., 2015), compared to that of the unreinforced ones.

Table 2 – Experimental results

Specimen	Maximum load H_{max}				Peak lateral displacement u_p				Ultimate lateral displacement u_u				
	Pos. [kN]	Neg. [kN]	Avg. [kN]	R_{load} [–]	Pos. [mm]	Neg. [mm]	Avg. [mm]	R_{disp} [–]	Avg. [mm]	u_u/h [–]	R_{disp} [–]	f_t [MPa]	R_t [–]
P-R2U	106.8	108.8	107.8	-	4.96	3.82	4.39	-	7.51	0.004	-	0.118	-
P-R2R-1	164.0	155.0	159.5	1.48	10.06	16.22	13.14	2.99	28.72	0.014	3.83	0.219	1.86
P-R2R-2	234.3	224.5	229.4	2.13	20.03	19.99	20.01	4.56	48.93	0.025	6.52	0.373	3.16

5. Three-point bending tests

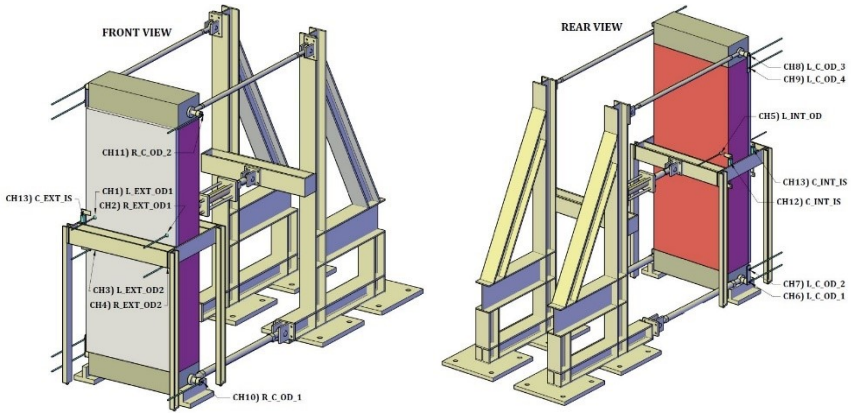

(a) (b)

Fig. 7. Front (a) and rear (b) view of the three-point bending test setup

The masonry specimen was laid over a reinforced concrete element with dimensions of 1.03 x 0.35 x 0.25 m^3, and through a C40 steel bar Ø50 mm L=1300 mm, embedded in the center of the concrete element, pin connected vertically to the base of the laboratory and horizontally to a stiff steel structure fixed to the base of the laboratory. A second RC element of the same dimensions was placed on the top of the masonry specimen, with a Ø40 mm steel bar embedded in the center of the beam that is pin connected to the same stiff steel structure. To apply the load, two HEA 160 steel beams, connected at the ends, were placed horizontally at both faces of the specimen at half height, kept in place by four vertical steel profiles moving on ball bearings. The hydraulic jack is placed at half height of the specimen, between a HEB 180 steel beam, fixed on the same stiff steel structure mentioned above.

Three-point bending experiments were carried out on the specimens by using a hydraulic jack, actioned by a manual pump, to apply horizontal forces at the mid-height section of the specimen. The actuator was moved cyclically with complete inversion, by considering a displacement-controlled test protocol until a certain damage was reached in the unreinforced side of the walls. The test was then completed monotonically towards the reinforced side until failure of the reinforcement occurred. Thirteen potentiometer displacement transducers were used to survey the displacements of each specimen, and a pressure transducer was installed on the jack hydraulic circuit to measure the horizontal load in both directions. The tested specimen B-R2 draft is presented in Fig. 8.

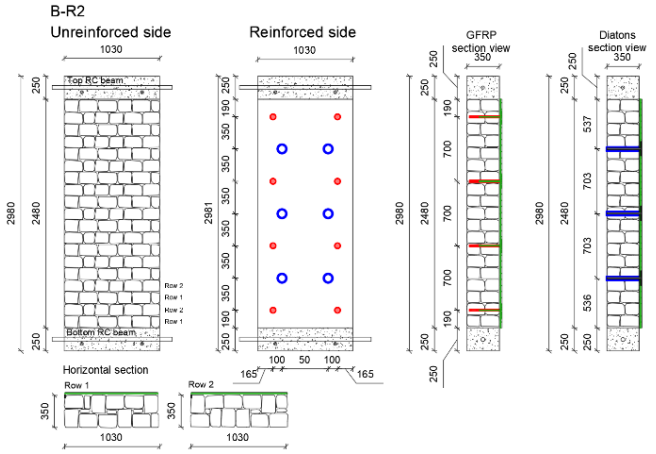

Fig. 8. Details of the unstrengthened specimen B-R2

During the test, on the unreinforced side it was noted a failure mechanism characterized by the opening of a nearly horizontal crack located just above the loading plate, at a relative average middle displacement u=-0.8 mm and a force of 4.9 kN. The test was conducted cyclically until a second horizontal crack formed at a displacement u=-22 mm. After this, the test was then conducted monotonically on the reinforced side, so as to prevent the mortar from falling from joints on the unreinforced side, decreasing the masonry compressive strength. The wall manifested a typical failure mechanism, on the strengthened side, characterized by the progressive opening and propagation of almost horizontal cracks in the reinforced coating of the specimen, leading to a subsequent collapse, due to also the progressive opening and propagation of diagonal cracks in the thickness of the wall, starting from the loading plate as a punching shear collapse.

The first crack on the reinforced side occurred at u=1.5 mm, horizontally at the height of the loading apparatus, while at u=3mm two almost specular horizontal cracks formed near the middle section, outside of the loading plate. Starting at u=22.0 mm, two diagonal cracks formed in the thickness of the wall, starting from the loading plate, due to punching shear and kept propagating in the following steps. At the end of the test, for a displacement of u=63.1 mm, the reinforcement had multiple, mostly horizontal cracks on the reinforced coating and the main crack opened at about ¾ of the masonry height. A progressive separation of the two wall leaves was registered during the test, with a final value of about 2.9 mm, meaning an in-thickness strain of about 7.6%.

The progressive formation of cracks during different steps on the front side of the specimen is reported in Fig. 9a, along with the configuration of the cracks at the end of the test (Fig. 9b, c).

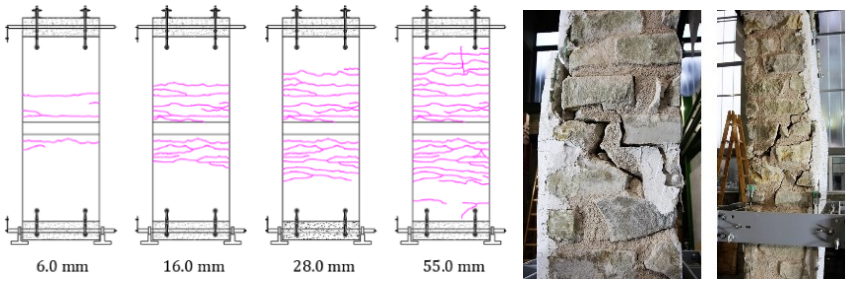

Fig. 9. Crack evolution on the reinforced coating of specimen B-R2 (a), crack configuration at the end of the test (b), (c)

In Fig. 10a the diagram representing the behavior of the reinforced side (I quadrant) and of the unreinforced side (III quadrant) is illustrated. The diagram describes what happens on both sides in terms of horizontal loads compared to the middle height out-of-plane average relative displacement. It can be easily evidenced the effectiveness of the reinforcement (a resistance eight times greater than the unreinforced sample and a displacement capacity more than three times that of the unstrengthen specimen). In Fig. 10b the specimen at the end of the test is presented.

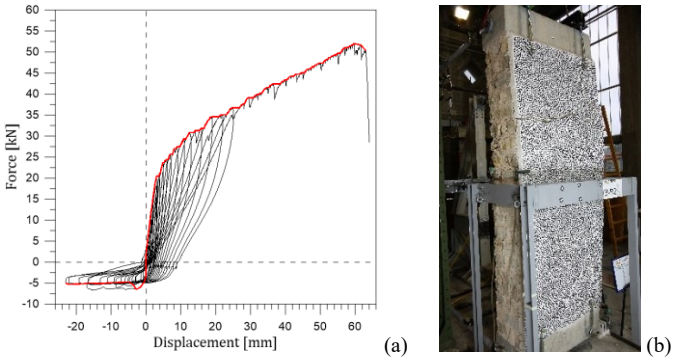

Fig. 10. Load (H) vs middle height average relative displacement (u) curve for specimen B-R2 (a), specimen appearance at the end of the test (b)

6. Conclusions

In the present paper the results of in-plane and out-of-plane experimental tests on stone masonry walls strengthened on one or two sides (shear-compression) and on one side (out-of-plane) were reported. Shear-compression test results evidenced a significant effectiveness with the two strengthening configurations of the CRM System. These values were obtained: increase by 48% in resistance and 280% in displacement capacity, with the reinforcement applied on one side of the specimen and diatones; increase by 113% in resistance and 550% in displacement capacity, with the reinforcement at both sides connected with L-shaped connectors. The results of the out-of-plane test has shown a consistent increase in resistance (700%) and in displacement capacity (200%), of the strengthened specimen compared with the values obtained from the equivalent unreinforced one. Furthermore, the collapse of the strengthened sample occurred at the composite GFRP mesh rupture.

This type of technology is, seeing the results obtained both on in-plane and out-of-plane tests, very efficient not only for strengthening, but also for providing an important displacement capacity (ductility).

Acknowledgements

The experimental tests presented have been developed within the project CONSTRAIN, funded by the Interreg Italy-Slovenia Cooperation Programme 2014-2020; leaded by the University of Trieste (Italy), alongside with the University of Ljubljana (Slovenija) and the companies FibreNet S.p.A., Igmat d.d., Veneziana Restauri Costruzioni S.r.l. and Kolektor CPG d.o.o..

References

Cascardi, A., Leone, M., Aiello, M.A., 2020. Transversal joining of multi-leaf masonry through different types of connector: Experimental and theoretical investigation. Construction and Building Materials 265, 120733.

De Santis, S., De Canio, G., de Felice, G., Meriggi, P., Roselli, I., 2019. Out-of-plane seismic retrofitting of masonry walls with Textile Reinforced Mortar composites. Bull Earthquake Eng 17.

Garcia-Ramonda, L., Pelà, L., Roca, P., Camata, G., 2022. Cyclic shear-compression testing of brick masonry walls repaired and retrofitted with basalt textile reinforced mortar. Composite Structures 283, 115068.

Gattesco, N., Amadio, C., Barelli, S., Bedon, C., Rinaldin, G., Zorzini, F., 2013. Studio numerico-sperimentale di pareti murarie in pietrame rinforzate mediante intonaco armato con rete in GFRP 13.

Gattesco, N., Amadio, C., Bedon, C., 2015. Experimental and numerical study on the shear behavior of stone masonry walls strengthened with GFRP reinforced mortar coating and steel-cord reinforced repointing. Engineering Structures 90, 143–157.

Guerreiro, J., Proença, J., Ferreira, J.G., Gago, A., 2018. Experimental characterization of in-plane behaviour of old masonry walls strengthened through the addition of CFRP reinforced render. Composites Part B: Engineering 148, 14–26.

Ismail, N., Ingham, J.M., 2016. In-plane and out-of-plane testing of unreinforced masonry walls strengthened using polymer textile reinforced mortar. Engineering Structures 118, 167–177.Mercedes, L., Bernat-Maso, E., Gil, L., 2020. In-plane cyclic loading of masonry walls strengthened by vegetal-fabric-reinforced cementitious matrix (FRCM) composites. Engineering Structures 221, 111097.

Valluzzi, M.R., Da Porto, F., Modena, C., 2001. Behaviour of multi-leaf stone masonry walls strengthened by different intervention techniques,11.